Supplementary material for:

Collapse-reexpansion conformational transition of alginate under non-specific ionic conditions

*Xiaoyang Li‡, Yi Wang‡, Cuixia Sun, Yiguo Zhao, Wei Lu, Yapeng Fang**

School of Agriculture and Biology, Shanghai Jiao Tong University, 800 Dongchuan Road, Shanghai 200240, China

Estimation of alginate concentration. To confirm the alginate concentration in our system is in dilute condition, where no interchain interaction have to be expected, the volume spanned by all the envelops of alginate chains was compared to the total sample volume (assumptions: WLC behavior of chains, homogeneous distribution of polymers within the sample, monodisperse system with average contour length $\langle L \rangle$):

$$\frac{V_{envelops}}{V_{sample}} = \frac{\frac{4}{3}\pi(\langle R_{3D} \rangle/2)^3 N_{chains}}{V_{sample}}$$

where V_{sample} = 1 mL = 1 cm^3 and $\langle R_{3D} \rangle$ is the average 3D end-to-end distance given by:

$$\langle R_{3D} \rangle = \left(2L_p\left(\langle L \rangle - L_p\left(1 - e^{\left(-\langle L \rangle / L_p\right)}\right)\right)\right)^{0.5}$$

where L_p is the persistence length and $\langle L \rangle$ is the contour length as extracted from AFM images.

And

$$N_{chains} = \frac{N_{units}}{\langle L \rangle / l_{unit}} = \frac{n_{units} \cdot N_A}{\langle L \rangle / l_{unit}}$$

where n_{units} [mol] = (1•10^{-6} [g•mL^{-1}] • 1 [mL])/M_{mono} [g•mol^{-1}] with M_{mono} =198 [g•mol^{-1}], N_A = 6.02•10^{23} [mol^{-1}], and l_{unit} = 0.5 nm. Based on these calculations, the ratio of $V_{envelops}/V_{sample}$ gives values below 0.003 for both ALG56 and ALG25 at each ionic strength, which is about two orders of magnitude below the volume fraction of random-close packed spheres, 0.64, from which interchain interactions are expected to start. Thus, our system (1 μg/mL) is in a very dilute state.

The overlap concentration (c^*) can also be used to demonstrate the dilute condition, which can be calculated as:

$$c^* = \frac{\langle L \rangle / l_{unit} {l_{unit}}^3}{(4/3)\pi(\langle R_{3D} \rangle/2)^3}$$

The result gives the c^* values above ~1•10^{-4} for ALG56 and ALG25 at all ionic strength, which is about two orders of magnitude larger than the concentration of alginate used, confirming again that interchain interaction can be neglected.

Supplementary Figures S1-S6:

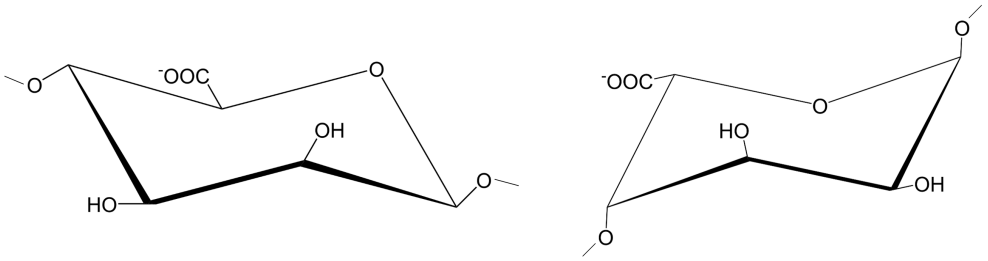

***β*-D-mannuronate (M)** ***α*-L-guluronate (G)**

Fig. S1. The repeating unit of alginate

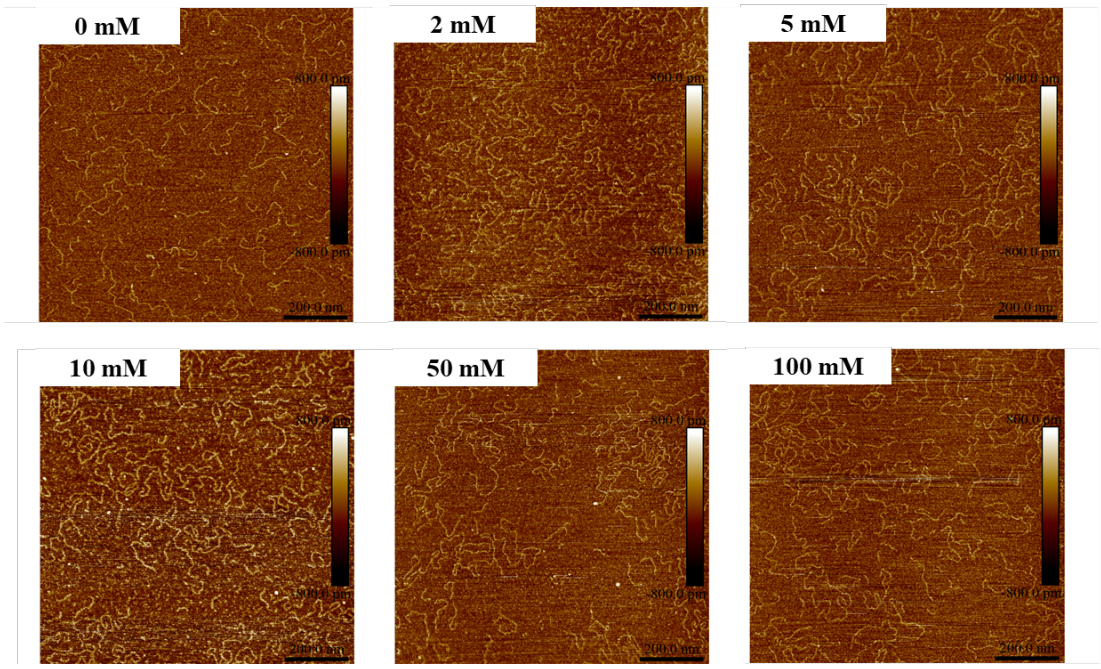

Fig. S2. AFM images of ALG25 at different NaCl concentrations.

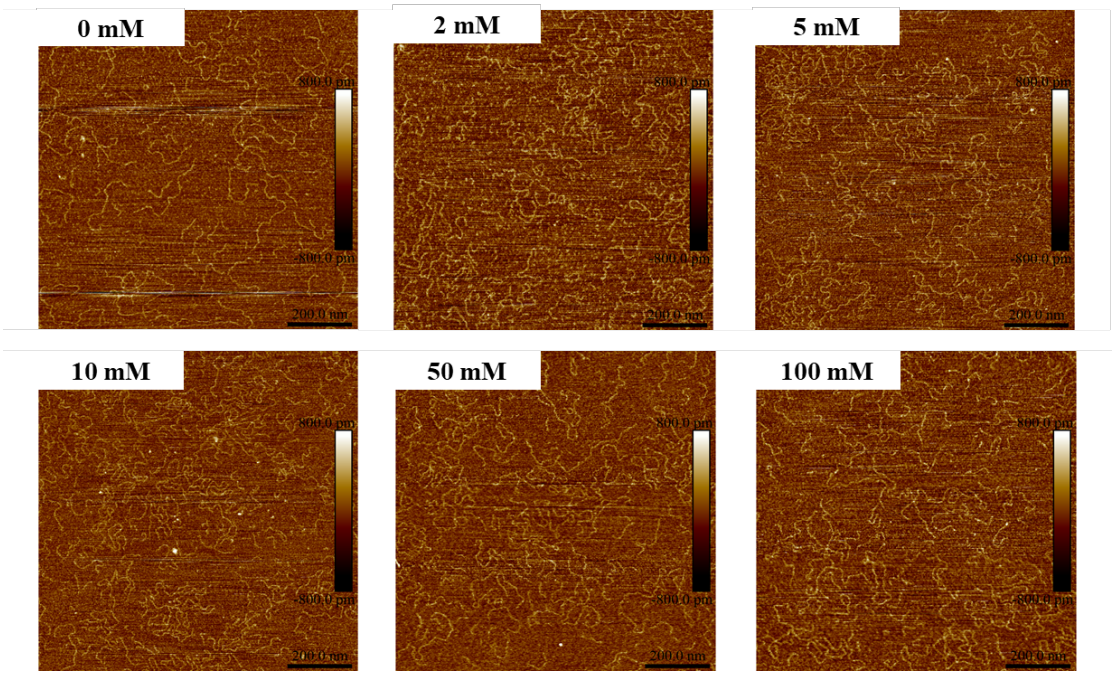

Fig. S3. AFM images of ALG25 at different KCl concentrations.

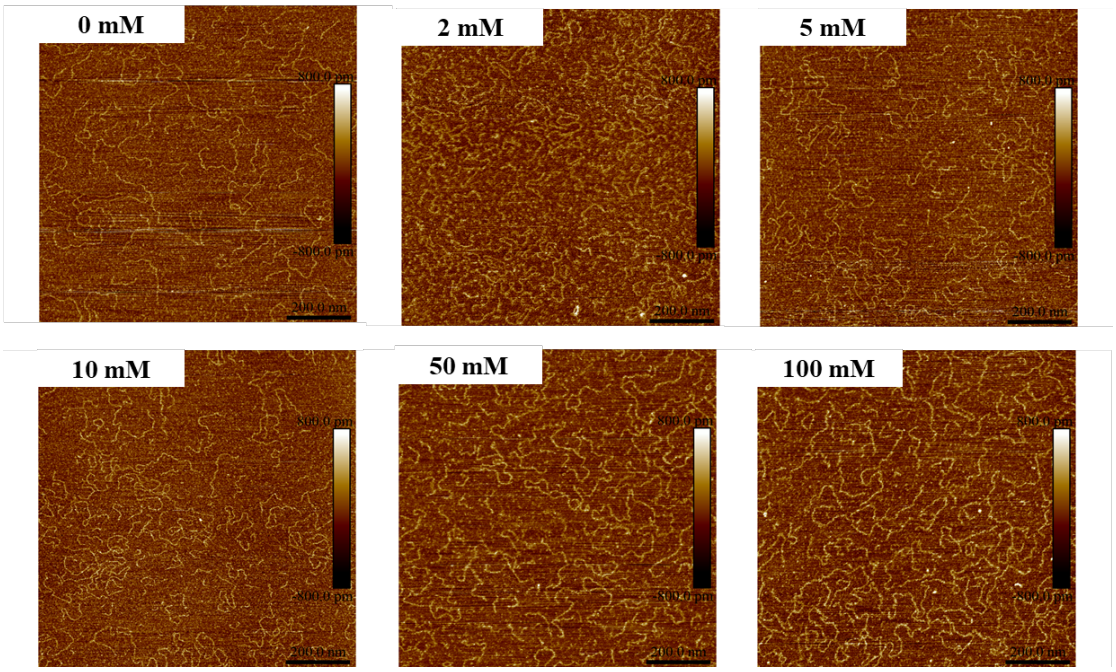

Fig. S4. AFM images of ALG25 at different $MgCl_2$ concentrations.

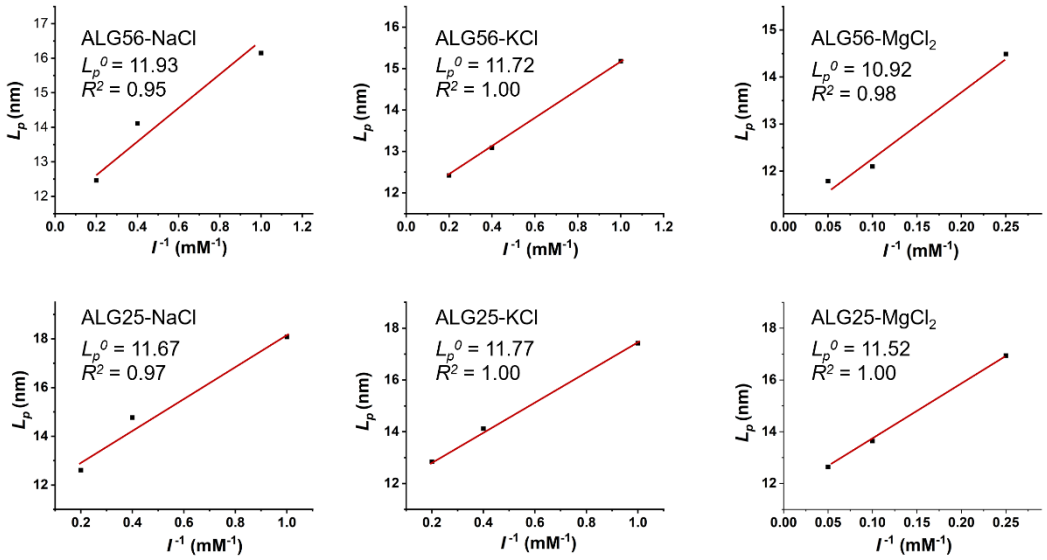

Fig. S5. The persistence length of ALG56 and ALG25 as a function of the reciprocal ionic strength.

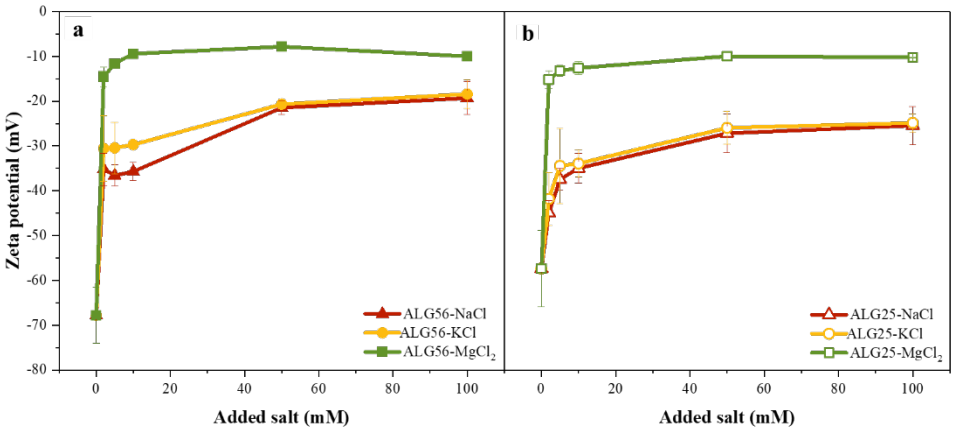

Fig. S6. Zeta potential of ALG56 (a) and ALG25 (b) solutions at different salt concentrations.

Table S1. The ion content of ALG6 and ALG25 before and after purification.

Ion content (w/w%)	Before purification		After purification	
	ALG56	ALG25	ALG56	ALG25
Na^{+}	10.24	9.81	8.10	7.90
K^{+}	0.04	0.06	0.03	0.05
Ca^{2+}	0.36	0.31	0.03	0.04
Mg^{2+}	0.02	0.02	0.01	0.03

Table S2. The mass fraction of alginate and added ions in the tested solutions.

M^{n+}	c (mM)	w_{ion} (w/w %)	w_{ALG} (w/w %)
Na^+	0	0	0.0001
	2	0.0046	0.0001
	5	0.0115	0.0001
	10	0.0230	0.0001
	50	0.1150	0.0001
	100	0.2300	0.0001
K^+	0	0	0.0001
	2	0.0078	0.0001
	5	0.0195	0.0001
	10	0.0390	0.0001
	50	0.1950	0.0001
	100	0.3900	0.0001
Mg^{2+}	0	0	0.0001
	2	0.0048	0.0001
	5	0.0121	0.0001
	10	0.0243	0.0001
	50	0.1215	0.0001
	100	0.2430	0.0001

Table S3. The structural information of alginate chains extracted from the AFM images, including the average height, <h>, the persistence length, L_p, and the electrostatic persistence length, L_p^e.

M^{n+}	c (mM)	ALG56			ALG25		
		<h> (nm)	L_p (nm)	L_p^e (nm)	<h> (nm)	L_p (nm)	L_p^e (nm)
Na^+	0	0.30	28.98	17.28	0.30	26.34	14.64
	2	0.30	16.15	4.45	0.30	18.08	6.38
	5	0.29	14.11	2.41	0.29	14.77	3.07
	10	0.31	12.46	0.76	0.31	12.61	0.91
	50	0.29	14.05	2.35	0.29	14.92	3.22
	100	0.33	14.35	2.65	0.30	15.45	3.75
K^+	0	0.30	28.98	17.28	0.30	26.34	14.64
	2	0.31	15.18	3.48	0.31	17.42	5.72
	5	0.31	13.09	1.39	0.29	14.12	2.42
	10	0.31	12.42	0.72	0.29	12.84	1.14
	50	0.32	15.50	3.80	0.30	16.95	5.25
	100	0.37	15.93	4.23	0.33	18.51	6.81
Mg^{2+}	0	0.30	28.98	17.28	0.30	26.34	14.64
	2	0.31	14.49	2.79	0.30	16.94	5.24
	5	0.33	12.10	0.40	0.31	13.64	1.94
	10	0.33	11.70	0.00	0.30	12.64	0.94
	50	0.33	18.96	7.26	0.35	19.90	8.20

	100	0.38	20.89	9.19	0.34	21.58	9.88